

Measurement of the $pn \rightarrow dK^+K^-$ total cross section close to threshold

Y. Maeda,^{1,*} M. Hartmann,^{2,3,†} I. Keshelashvili,⁴ S. Barsov,⁵ M. Büscher,^{2,3} A. Dzyuba,⁵ S. Dymov,^{6,7} V. Hejny,^{2,3} A. Kacharava,^{2,3} V. Kleber,⁸ V. Koptev,⁵ P. Kulesa,⁹ T. Mersmann,¹⁰ S. Mikirtytchians,^{2,3,5} A. Mussgiller,⁷ M. Nekipelov,^{2,3} H. Ohm,^{2,3} K. Pysz,⁹ H.J. Stein,^{2,3} H. Ströher,^{2,3} Yu. Valdau,⁵ C. Wilkin,¹¹ and P. Wüstner¹²

¹Research Center for Nuclear Physics, Osaka University, Ibaraki, Osaka 567-0047, Japan

²Institut für Kernphysik, Forschungszentrum Jülich GmbH, 52425 Jülich, Germany

³Jülich Centre for Hadron Physics, 52425 Jülich, Germany

⁴Department of Physics, University of Basel, Klingelbergstrasse 82, 4056 Basel, Switzerland

⁵High Energy Physics Department, Petersburg Nuclear Physics Institute, 188350 Gatchina, Russia

⁶Laboratory of Nuclear Problems, Joint Institute for Nuclear Research, 141980 Dubna, Russia

⁷Physikalisches Institut II, Universität Erlangen–Nürnberg, 91058 Erlangen, Germany

⁸Physikalisches Institut, Universität Bonn, 53115 Bonn, Germany

⁹H. Niewodniczański Institute of Nuclear Physics PAN, 31342 Kraków, Poland

¹⁰Institut für Kernphysik, Universität Münster, 48149 Münster, Germany

¹¹Physics and Astronomy Department, UCL, Gower Street, London WC1E 6BT, UK

¹²Zentralinstitut für Elektronik, Forschungszentrum Jülich GmbH, 52425 Jülich, Germany

(Dated: October 15, 2018)

Measurements of the $pd \rightarrow p_{\text{sp}}dK^+K^-$ reaction, where p_{sp} is a spectator proton, have been undertaken at the Cooler Synchrotron COSY–Jülich by detecting a fast deuteron in coincidence with a K^+K^- pair in the ANKE facility. Although the proton beam energy was fixed, the moving target neutron allowed values of the non-resonant quasi-free $pn \rightarrow dK^+K^-$ total cross section to be deduced up to an excess energy $\epsilon \approx 100$ MeV. Evidence is found for the effects of K^-d and $KK\bar{K}$ final state interactions. The comparison of these data with those of $pp \rightarrow ppK^+K^-$ and $pp \rightarrow dK^+\bar{K}^0$ shows that all the total cross sections are very similar in magnitude.

PACS numbers: 25.40.Ve, 13.75.Cs, 14.40.Cs

We have recently published measurements of the differential and total cross sections for the $pp \rightarrow ppK^+K^-$ reaction at three energies close to threshold [1]. A major challenge in the analysis was the separation of the contribution from the production and decay of the ϕ meson from that of the non- ϕ component [2]. One of the striking features of the non- ϕ results is the strong attraction between the K^- and each of the final protons seen in the differential distributions. This also has a major effect on the energy dependence of the total cross section, enhancing it at low energies. Although tantalizing, these results do not, however, resolve the ongoing question as to whether the interaction is sufficiently strong to allow the K^- to form a bound state with the two protons [3, 4, 5].

The isospin dependence of ϕ production has been studied through an investigation of $pd \rightarrow p_{\text{sp}}dK^+K^-$ [6]. By identifying the final deuteron and kaon pair and measuring their momenta, it was possible to construct the momentum of the recoil proton p_{sp} to show that it was consistent with being a *spectator*, whose only significant participation in a reaction is through a change in the kinematics. Interpreting the results in this way, it was possible to extract values of the quasi-free $pn \rightarrow dK^+K^-$ cross section. Moreover, although the experiment was carried out at one fixed beam energy, the movement of the target neutron enabled data to be obtained over a wide range of excess energy $\epsilon = \sqrt{s} - m_d - 2m_K$ on an event-by-event basis. Just as in the $pp \rightarrow ppK^+K^-$ case, the shape of the K^+K^- invariant mass distribution

was used to separate the ϕ component from the non- ϕ background. The invariant K^+K^- mass spectrum for all events above the ϕ threshold is to be found in Ref. [6] and from this it is already seen that the non- ϕ contribution is a much smaller fraction of the total than in the $pp \rightarrow ppK^+K^-$ case [1]. The prime purpose of this work is to present the data on the energy dependence of the non- ϕ total cross section up to an excess energy of $\epsilon \approx 100$ MeV.

Unlike ϕ production, there are two different $pn \rightarrow dK^+K^-$ isospin channels. The $I = 1$ has already been investigated in some detail through the measurement of $pp \rightarrow dK^+\bar{K}^0$ at two beam energies, corresponding to $\epsilon = 47$ and 105 MeV [7, 8]. The identical nature of the initial protons, combined with angular momentum and parity conservation laws, demands that the $dK^+\bar{K}^0$ final state must contain at least one p -wave. At low energies this will suppress the $I = 1$ contribution to $pn \rightarrow dK^+K^-$ compared to $I = 0$ where there is no such constraint. As a consequence, the energy dependence of the $pn \rightarrow dK^+K^-$ total cross section is expected to be more complicated than that of $pp \rightarrow ppK^+K^-$.

The investigation was carried using a 2.65 GeV proton beam incident on an internal target of the Cooler Synchrotron COSY. The experimental details and the identification of the dK^+K^- candidates were described for ϕ production [6] and so we can here be very brief. The forward-going deuteron was measured in the ANKE magnetic spectrometer [9] and both charged kaons were

identified in coincidence on the basis of time-of-flight criteria. After putting a $\pm 3\sigma$ cut around the missing mass of the spectator proton, about 4500 $p_{\text{sp}}dK^+K^-$ events were recorded. The background from misidentified $p\pi^+\pi^-$ events was estimated to be less than 7% and effects from this were included in the systematic uncertainties.

The identification of the residual proton as a spectator is supported by its momentum distribution shown in Fig. 1(a), which follows well the prediction based upon the Bonn wave function [10].

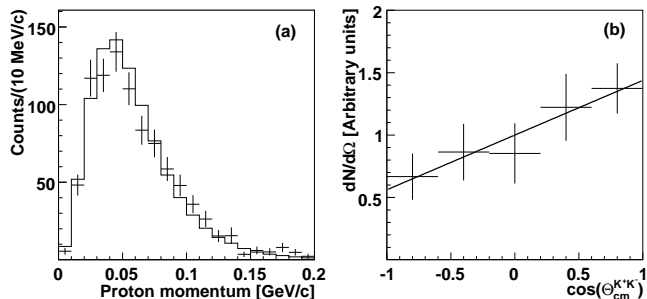


FIG. 1: (a) Spectator momentum distribution of non- ϕ events compared to simulation using the Bonn potential [10]. (b) Acceptance-corrected angular dependence of the polar angle of the K^+K^- system relative to the beam axis in the overall c.m. system at $12 < \epsilon < 32$ MeV. The data are well described by $1+0.4 \cos \theta$ (solid line).

The effective target density was determined by measuring the frequency shift of the stored proton beam as it lost energy due to its repeated passages through the target [11, 12]. Combining this with a measurement of the beam current, an integrated luminosity of $(23 \pm 1.4) \text{ pb}^{-1}$ was found over the 300 hours of data-taking.

The excess energy determined through the measurement of the momenta of the deuteron and the two kaons had a standard deviation that was typically $\sigma_\epsilon \approx 2$ MeV, which is small compared to the 10 MeV bins that were used in the subsequent data analysis. In order to evaluate the cross section in one of these ϵ intervals, the geometrical acceptance, resolution, detector efficiency and kaon decay probability were taken into account in a Monte Carlo simulation, using the GEANT4 program [13]. The fraction of the total luminosity falling within this interval was estimated from the deuteron Fermi momentum distribution predicted using the Bonn potential [10].

In the first step of the analysis, the distributions previously published [6] were taken as the basis of the simulation of the ϕ -production. For the non- ϕ component, three-body phase space was used. At each excess energy, the four independent c.m. distributions generated were chosen to be the K^+K^- invariant mass as well as three angular distributions. These were then divided into two groups, depending on the value of the K^+K^- invariant mass, *i.e.*, a ϕ -rich region where $1.05 < M(K^+K^-) < 1.35 \text{ GeV}/c^2$ with the remainder being designated as the

ϕ -poor region. All distributions were jointly fitted to the experimental data and the relative contribution of ϕ and non- ϕ production evaluated in order to determine the two acceptances.

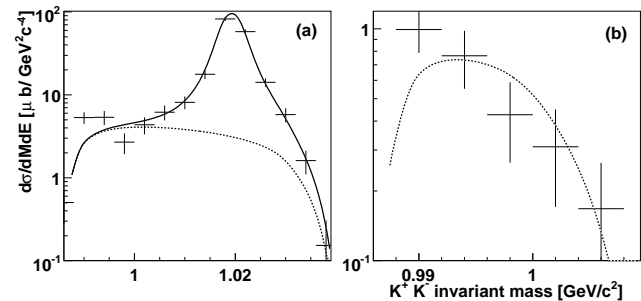


FIG. 2: K^+K^- invariant mass distributions of the $pn \rightarrow dK^+K^-$ reaction for event samples below and above the ϕ threshold. The data are shown for excess energy bins (a) $42 < \epsilon < 52$ MeV, and (b) $12 < \epsilon < 22$ MeV. The non- ϕ simulation (dashed curve) includes the effect of the K^-d *fsi*. The solid curve includes also a contribution from ϕ production, where applicable.

In the ϕ -poor region, the polar angle of the K^+K^- system relative to the beam axis in the overall c.m. system shows a forward peak for $\epsilon < 52$ MeV and a typical acceptance-corrected distribution is shown in Fig.1(b). The forward/backward asymmetry is evidence for some $I = 0/I = 1$ interference. The angular distribution for the ϕ -rich region is fairly symmetrical because of the $I = 0$ dominance and the lack of interference between the ϕ and the background. Fitting the shape with $1 + \alpha \cos \theta$, one finds $\alpha = 0.4 \pm 0.1$ at low energies but α consistent with zero at higher ϵ . Taking α to have the polynomial energy dependence on ϵ , its inclusion increases the total acceptance for non- ϕ production up to 8.5%. In addition, as discussed below, the $K^\pm d$ invariant masses deviate from phase space due to the strong final state interaction between K^- and deuteron (Fig. 3). This was included through a K^-d enhancement factor based on a scattering length approximation [8]. The deviations were taken into account iteratively in the simulations in order to converge on acceptance-corrected distributions.

Two typical K^+K^- mass spectra from above and below the ϕ threshold are shown in Fig. 2 after making acceptance and other corrections. Also illustrated there are fits to the ϕ and non- ϕ contributions to the cross section where, in the latter case, a distorted three-body phase space has been assumed for the dK^+K^- final state. In general the ϕ contribution is well described but the same cannot be said for the non- ϕ distribution. The difficulties here arise principally from the unknown fraction of p -waves that come from the $I = 1$ cross section and the influence of the K^-d final state interaction. In addition, for invariant masses below about $995 \text{ MeV}/c^2$, the data in Fig. 2(a) lie well above the simulation. This feature,

which is also seen quite clearly in the $pp \rightarrow ppK^+K^-$ data [1, 14], is evidence for a final state interaction in the $K\bar{K}$ subsystem. In the region of the $K^0\bar{K}^0$ threshold, the $K^+K^- \rightleftharpoons K^0\bar{K}^0$ coupling can lead to a cusp effect [15].

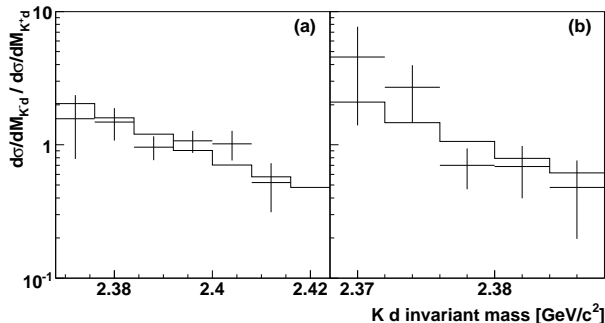


FIG. 3: Ratios of the $K^\pm d$ invariant mass distributions for the same two ranges of excess energy as in Fig. 2. (a): $42 < \epsilon < 52$ MeV, (b): $12 < \epsilon < 22$ MeV. The histograms are the simulations in the scattering length approximation with $a = (-1.0 + i1.2)$ fm.

Of much more importance for the acceptance estimation is the distortion in the K^-d subsystem. Figure 3 shows the ratio of the differential cross sections

$$R_{Kd} = \frac{d\sigma/dM(K^-d)}{d\sigma/dM(K^+d)} \quad (1)$$

for the non- ϕ region at the same excess energies as those shown in Fig. 2. Here $M(K^\pm d)$ is the invariant mass of the $K^\pm d$ subsystem. Experimental distributions of R_{Kd} at both energies show a very strong preference for low values of $M(Kd)$, which arises from the interaction between K^- and deuteron. A K^-d final state interaction factor is introduced into the three-body phase space simulation of the non- ϕ contribution by using the scattering length approximation $1/(1 - iqa)$, where q is the K^-d relative momentum. The (complex) scattering length is believed to be of the order of $a \approx (-1.0 + i1.2)$ fm [16], which would correspond a bound or virtual state with a binding energy of $\epsilon_0 \approx 20$ MeV. The ANKE $pp \rightarrow dK^+\bar{K}^0$ data seem to be insensitive to the phase of a but they are best fit with $|a| \approx 1.5$ fm [8]. After taking $a = (-1.0 + i1.2)$ fm, the individual $d\sigma/dM(K^+d)$ and $d\sigma/dM(K^-d)$ distributions are well described, as is the ratio R_{Kd} , which is shown for the two excess energy intervals by the histograms in Fig. 3.

In view of the low statistics and the consequent fluctuations, the non- ϕ total cross section in a ϵ bin was evaluated in two different ways, (a) by subtracting the fit to the ϕ component in Fig. 2 and summing the remainder, and (b) by taking the direct fit to the non- ϕ part of Fig. 2. The average of these two values is given as the total cross section in Table I. The difference is a major contributor to the systematic uncertainties given there.

TABLE I: Total cross section for the non- ϕ component of the $pn \rightarrow dK^+K^-$ reaction as a function of the excess energy ϵ with respect to the dK^+K^- threshold. The first error on the cross section is statistical and the second systematic whereas that on the energy is the bin half-width. The overall $\approx \pm 6\%$ uncertainty in the luminosity has not been compounded with the other errors.

ϵ (MeV)	$\sigma_{\text{non-}\phi}(\text{tot})$ (nb)
17.1 ± 5.0	$1.8 \pm 0.3 \pm 0.1$
27.1 ± 5.0	$5.9 \pm 1.0 \pm 0.7$
37.1 ± 5.0	$12.4 \pm 2.5 \pm 1.8$
47.1 ± 5.0	$16.2 \pm 3.6 \pm 1.9$
57.1 ± 5.0	$27.6 \pm 4.8 \pm 3.2$
67.1 ± 5.0	$34.9 \pm 6.7 \pm 3.4$
77.1 ± 5.0	$38.6 \pm 10.0 \pm 5.0$
87.1 ± 5.0	$50.2 \pm 14.3 \pm 7.7$
102.1 ± 10.0	$69.5 \pm 17.5 \pm 10.7$

The values of the $pn \rightarrow dK^+K^-$ total cross section presented in Fig. 4 shows a smooth behavior on a logarithmic scale. Also shown are results for the $pp \rightarrow ppK^+K^-$ [1, 14, 17] and $pp \rightarrow dK^+\bar{K}^0$ [7].

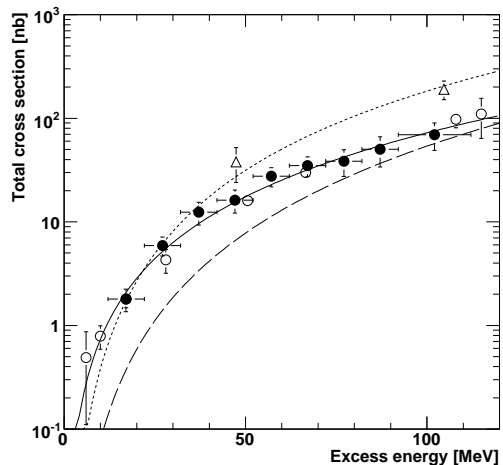


FIG. 4: Total cross section for non- ϕ $K\bar{K}$ production in nucleon-nucleon collisions near threshold. The closed circles denote $pn \rightarrow dK^+K^-$ data (this work) and $pp \rightarrow dK^+\bar{K}^0$ (open triangles [7]), whereas the open circles show the results for $pp \rightarrow ppK^+K^-$ from Refs. [1, 14, 17]. The dotted curve is the best fit of Eq. (3) to the $pp \rightarrow dK^+\bar{K}^0$ data whereas the solid curve includes also the isospin-zero contribution of Eq. (3) so as to describe the energy dependence of the $pn \rightarrow dK^+K^-$ total cross section. The dashed curve represents the subsequent prediction of Eq. (4) for the $pn \rightarrow \{pn\}_{I=0}K^+K^-$ total cross section.

The isospin dependence of kaon pair production can be deduced from

$$\begin{aligned} \sigma(pp \rightarrow dK^+\bar{K}^0) &= \sigma_1, \\ \sigma(pn \rightarrow dK^+K^-) &= \frac{1}{4}(\sigma_1 + \sigma_0). \end{aligned} \quad (2)$$

Interpolating our results to the energies where the $pp \rightarrow dK^+\bar{K}^0$ has been studied [7], we find isospin ratios of $\sigma_0/\sigma_1 = 0.9 \pm 0.9$ at 47 MeV and 0.5 ± 0.5 at 105 MeV. The large error bars arise from the subtraction implicit in Eq. (2) and it is hard to draw firm conclusions except that σ_0 cannot be much larger than σ_1 . There might be a tendency for σ_1 to become relatively more important as the energy is raised. This is what one would expect from the requirement of having a p -wave in the $pp \rightarrow dK^+\bar{K}^0$ final state [7, 8].

A major influence on the energy dependence of the total cross section arises from the K^-d final state interaction which gives the distortion shown in Fig. 3. Although the closed form description of Ref. [18] is only strictly valid for a real scattering length, to a good approximation the energy dependence of the two cross sections should be given by

$$\begin{aligned}\sigma_0 &= A_0 \epsilon^2 / D, \\ \sigma_1 &= A_1 \epsilon^3 (D + \frac{1}{2}\epsilon/\epsilon_0) / D^2, \\ D &= \left(1 + \sqrt{1 + \epsilon/\epsilon_0}\right)^2,\end{aligned}\quad (3)$$

where $\epsilon_0 \approx 20$ MeV.

The choice of the $I = 0$ and $I = 1$ coefficients $A_0 = 127$ pb/MeV² and $A_1 = 1.8$ pb/MeV³ leads to the fits to the $pp \rightarrow dK^+\bar{K}^0$ and $pn \rightarrow dK^+K^-$ total cross sections shown in Fig. 4. The general behavior is reproduced much better than it would be if the K^-d final state interaction were neglected.

Another important feature of Fig. 4 is that the $pp \rightarrow ppK^+K^-$ and $pn \rightarrow dK^+K^-$ total cross sections are similar in magnitude. However some allowance has to be made for the four-body nature of the ppK^+K^- phase space. An estimate of this effect can be obtained in a simple final state interaction model [19]. This predicts that

$$\begin{aligned}\sigma(pn \rightarrow \{pn\}_{I=0}K^+K^-) / \sigma(pn \rightarrow dK^+K^-) \approx \\ \frac{2}{\pi\sqrt{x}} \left[\frac{5}{6} + \frac{4x}{15} + \frac{1}{2x} - 2\sqrt{x} \left(\frac{1+x}{2x} \right)^2 \arctan\sqrt{x} \right],\end{aligned}\quad (4)$$

where $x = \epsilon/B$, with B denoting the deuteron binding energy. The result of multiplying this ratio by the fit to the $pn \rightarrow dK^+K^-$ total cross section is shown in Fig. 4. Using this simple estimate we see that

$$\sigma(pp \rightarrow ppK^+K^-) / \sigma(pn \rightarrow \{pn\}_{I=0}K^+K^-) \approx 1.5. \quad (5)$$

It is clear from the results presented here that, after correcting for the different phase spaces, the total cross sections for the $pp \rightarrow ppK^+K^-$, $pn \rightarrow dK^+K^-$, and $pp \rightarrow dK^+\bar{K}^0$ reactions are very similar in magnitude despite the necessity for p -waves in the last case. It would be highly desirable to have a common theoretical model to describe all three channels.

We are grateful for the support offered by the COSY machine crew and other members of the ANKE Collaboration. This work has been partially financed by the BMBF, DFG, Russian Academy of Sciences, HGF-VIQCD, and COSY FFE.

* E-mail: ymaeda@rcnp.osaka-u.ac.jp

† E-mail: M.Hartmann@fz-juelich.de

- [1] Y. Maeda *et al.*, Phys. Rev. C **77**, 015204 (2008).
- [2] M. Hartmann *et al.*, Phys. Rev. Lett. **96**, 242301 (2006).
- [3] M. Agnello *et al.*, Phys. Rev. Lett. **94**, 212303 (2005).
- [4] T. Yamazaki and Y. Akaishi, Phys. Rev. C **76**, 045201 (2007).
- [5] N.V. Shevchenko, A. Gal, J. Mareš, J. Révai, Phys. Rev. C **76**, 044004 (2007).
- [6] Y. Maeda *et al.*, Phys. Rev. Lett. **97**, 142301 (2006).
- [7] V. Kleber *et al.*, Phys. Rev. Lett. **91**, 172304 (2003); A. Dzyuba *et al.*, Eur. Phys. J. A **29**, 245 (2006)
- [8] A. Dzyuba *et al.*, Eur. Phys. J. A **38**, 1 (2008).
- [9] S. Barsov *et al.*, Nucl. Instrum. Methods Phys. Res. A **462**, 364 (2001).
- [10] R. Machleidt, K. Holinde, and Ch. Elster, Phys. Rep. **149**, 1 (1987).
- [11] K. Zapfe, Nucl. Instrum. Methods Phys. Res. A **368**, 293 (1996).
- [12] H.J. Stein *et al.*, Phys. Rev. ST Accel. Beams, **11**, 052801 (2008).
- [13] S. Agostinelli *et al.*, Nucl. Instrum. Meth. A **506**, 250 (2003); <http://geant4.web.cern.ch/geant4/>
- [14] F. Balestra *et al.*, Phys. Rev. C **63**, 024004 (2001).
- [15] A. Dzyuba *et al.*, Phys. Lett. B **668**, 315 (2008).
- [16] U.-G. Meißner, U. Raha, A. Rusetsky, Eur. Phys. J. C **47**, 473 (2006).
- [17] M. Wolke, PhD thesis, University of Münster (1997); C. Quentmeier *et al.*, Phys. Lett. B **515**, 276 (2001); P. Winter *et al.*, Phys. Lett. B **635**, 23 (2006).
- [18] G. Fäldt and C. Wilkin, Phys. Lett. B **382**, 209 (1996).
- [19] C. Wilkin, U. Tengblad, and G. Fäldt, Acta Physica Slovaca **56**, 205 (2006).